Accepted Manuscript

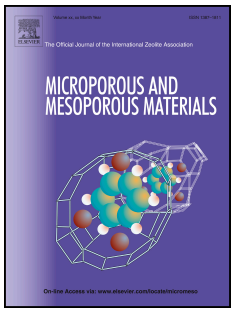

Microporous frameworks with conjugated π-electron skeletons for enhanced gas and organic vapor capture

Jianwei Guo, Xiong Li, Shuqin Fu, Rui Tong, Paul D. Topham, Jiawei Wang

PII: S1387-1811(18)30131-8

DOI: 10.1016/j.micromeso.2018.03.007

Reference: MICMAT 8823

To appear in: *Microporous and Mesoporous Materials*

Received Date: 6 December 2017

Revised Date: 6 March 2018

Accepted Date: 10 March 2018

Please cite this article as: J. Guo, X. Li, S. Fu, R. Tong, P.D. Topham, J. Wang, Microporous frameworks with conjugated π-electron skeletons for enhanced gas and organic vapor capture, *Microporous and Mesoporous Materials* (2018), doi: 10.1016/j.micromeso.2018.03.007.

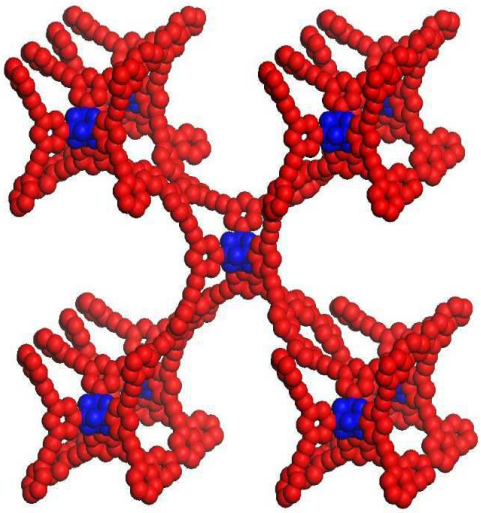

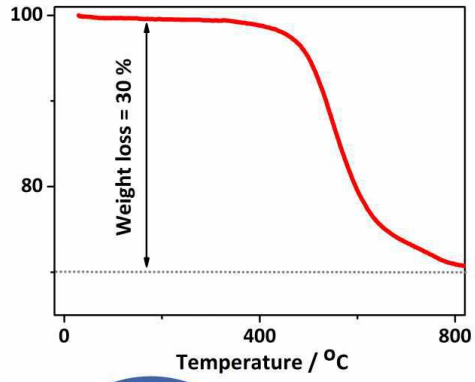

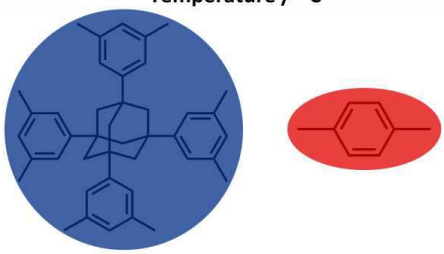

Microporous frameworks with conjugated π-electron skeletons for enhanced gas and organic vapor capture

Jianwei Guo,[a]* Xiong Li,[a] Shuqin Fu,[a] Rui Tong,[b] Paul D Topham,[c]* Jiawei Wang[c]

Abstract: Novel conjugated microporous frameworks based on adamantane (**CMF-Ad**s) have been successfully synthesized under mild conditions. Eight-arm tetraphenyl "knots" and a conjugated π-electron skeleton endowed the target **CMF-Ad**s with ultra-high thermal stability (up to 500 ^{o}C), high surface area (up to 907 m^2 g^{-1}), excellent CO_2 uptake capacity of 15.13 wt % at 273 K and 1 bar, as well as superior organic vapor (benzene, hexane) adsorption. The ultra-high gas uptake capacity and selectivity of these **CMF-Ad**s herein exceeds most conjugated microporous frameworks reported to date, highlighting their potential as materials for clean energy application.

Keywords: conjugated microporous frameworks, carbon-dioxide capture, selectivity, π-conjugated skeletons, adamantane

Carbon dioxide capture and sequestration (CCS) and capture of volatile organic compounds (VOCs) from post-combustion effluents have emerged as two of the most significant challenges facing mankind today.[1, 2] Porous organic materials, which exhibit high tailor-made functionality and flexibility through molecular design, gain enormous scientific attention as gas adsorbents due to their high surface area, low framework density, as well as high gas sorption capacities relying on physical adsorption and low regeneration energy consumption.[3, 4] To date, extensive work has been reported on conjugated microporous polymers (CMPs)[5], where the rich conjugated π-electron skeleton differentiates them from other porous organic materials. Owing to high surface area and tunable microporous size, CMPs are considered to be powerful platforms for CO_2 capture. Additionally, it has been demonstrated that microporous organic materials that combine π-conjugated skeletons with a permanent nanoporous structure could increase CO_2 capacity due to the interaction between the quadrupole moments of CO_2 and the π-clouds in the materials.[6-9] However, the building blocks of CMPs have been limited to planar π-system molecules, such as riazine[10] and polycarbazole.[11, 12] Furthermore, structural stacking in the solid state reduces interaction between CO_2 molecule and porous materials, severely restricting CO_2 uptake. Thus, designing novel porous networks with high surface area, rich conjugated π-electron skeleton and high physicochemical stability toward CO_2 capture is a continued pressing challenge.

Herein, we report a strategy for the design and construction of novel conjugated microporous frameworks based on π-conjugated building blocks. Rigid 1,3,5,7-tetrakis(1,3-bibromophenyl)adamantane (TBBPA), reported here for the first time, has been employed as an integral feature in the design of conjugated microporous adamantane-based frameworks (**CMF-Ad**s) *via* Suzuki cross coupling reactions under argon atmosphere, as depicted in Fig. S1 (a). The yields for the three structurally related **CMF-Ad** networks synthesized herein (see Fig. 1) were 95.1 %, 90.8 % and 87.7 %, respectively, based on hypothetical 100 % polycondensation. The introduction of TBBPA equips the CMPs with high surface area, high physicochemical stability, rich conjugated π-electron threads running through the skeletons, as well as excellent gas uptake capacity, including H_2, CO_2 adsorption and CO_2/CH_4 selectivity.

The three novel **CMF-Ad** networks were shown to be insoluble and stable in common organic solvents, such as ethanol, chloroform and tetrahydrofuran, *etc.* Elemental analysis, FTIR and solid state ^{13}C CP/MAS NMR spectroscopy were used to confirm the structure of these **CMF-Ad** networks, revealing that the three desired π-conjugated frameworks were synthesized successfully. The FTIR spectra for all networks [Fig. S3 (ESI)] show a broad band near 3432 cm^{-1} indicating the presence of B-OH end-group vibrations. Typical C≡C vibrations at 2202 cm^{-1} are observed for **CMF-Ad-3** only, as expected. The results of ^{13}C CP/MAS NMR spectroscopy also confirmed the successful construction of the frameworks with TBBPA and diboronic acid. All detailed assignments of the resonances for particular carbon types are provided in Fig. S4 (ESI) and Table S1 (ESI). Thermogravimetric Analysis [TGA, Fig. 1 (b)] shows that **CMF-Ad-1** and **CMF-Ad-2** were thermally stable up to approximately 500 ^{o}C in a nitrogen atmosphere, significantly higher than most commonly reported frameworks,[13, 14] which is attributed to the 3D adamantane and aromatic structure.[15, 16] **CMF-Ad-3** degraded around 420 ^{o}C as a the result of the introduction of the alkyne groups. It is noteworthy that the high thermochemical stability of these frameworks is beneficial in post-combustion CO_2 capture which occur at high temperatures or within harsh environments.[17] The surface morphology of these frameworks (ESI, Fig. S5) was probed by scanning electron microscopy (SEM), showing particle-like morphology with an irregular shape and rough surface. This particle-like morphology is in

line with previously reported microporous frameworks based on adamantane.[15, 18] The broad features in the powder X-ray diffraction (XRD) patterns (ESI, Fig. S6) imply that these frameworks are non-ordered and more amorphous in nature. Solid state UV-vis and photoluminescence spectra (ESI, Fig. S7 and Fig S8) reveal that the electronic character of the framework can be through molecular design of the aryl borate building block (the so-called 'rods' of the framework). Further, the **CMF-Ad** networks showed emission bands at 398-540 nm[14] and suspensions of the frameworks in CH_2Cl_2 exhibited similar emissive colors (ESI, Fig. S9).

The porosity of the **CMF-Ad** networks were measured by cryogenic N_2 adsorption/desorption experiments at 77 K. According to the IUPAC definition,[9] the adsorption/desorption isotherms at 77 K give rise to mainly type I isotherms (Fig. 2). The steep uptake of N_2 at relatively low pressure ($p/p_0 < 0.01$) in our frameworks indicate that they are mainly microporous materials.[19, 20] Furthermore, the increase in N_2 adsorption above $p/p_0 = 0.9$ (for **CMF-Ad-1** and to a lesser extent **CMF-Ad-3**) is attributed to the interparticulate porosity, as seen from the cavities between agglomerated nanosphere (ESI, Fig. S5). The porous properties of these three networks are summarized in Table S2 (ESI). **CMF-Ad-1** shows the highest BET surface area (up to 907 $m^2 g^{-1}$) among the obtained networks, followed by **CMF-Ad-2** (up to 765 $m^2 g^{-1}$) and **CMF-Ad-3** (up to 604 $m^2 g^{-1}$). As three different length rods were used, the pore sizes should be different across our series of materials. "Extended" rigid rods should furnish the frameworks with larger pores, *i.e.* **CMF-Ad-3** should exhibit larger pores than **CMF-Ad-2**, which should, in turn, have larger than **CMF-Ad-1**. According to the pore size distributions (PSD) (Fig. 2 and Table S2 in ESI), **CMF-Ad-1** exhibited a smaller average micropore diameter than **CMF-Ad-2**, which was smaller than **CMF-Ad-3**, as predicted from the size of the molecular building blocks. Additionally, two different, closely size-related populations were observed for each network, most notably for **CMF-Ad-3**, suggesting the formation of interpenetrating networks during polymerization. Similar results were obtained for other reported CMFs.[21-23] The hysteresis for the three **CMF-Ad** networks over the measured range of relative pressure is believed to arise, in part, from the interparticulate porosity.

Frameworks with a narrow pore size of less than 1.0 nm and a π-conjugated skeleton are beneficial for gas sorption, inspiring the evaluation of their applicability in gas storage/purification. The small gas (H_2, CO_2, N_2 and CH_4) uptake of these frameworks were investigated up to 1.0 bar at 77 K (for H_2) and 273 K. As shown in Fig. 3 (a)-(d), the isothermal adsorption for H_2, CO_2, N_2 and CH_4 were demonstrates that the three frameworks possess excellent gas uptake capability. The H_2 uptake capacities for these frameworks were up to 1.44 wt % at 77 K and 1.0 bar, whereas CO_2 uptake capacities were up to 15.13 wt % at 273 K and 1.0 bar. These values surpass most microporous organic materials with comparable or even ultrahigh surface area, such as COF-103 (7.6 wt % for CO_2 uptake, 3530 $m^2 g^{-1}$),[20] microporous network A (11.7 wt % for CO_2 uptake, 4077 $m^2 g^{-1}$),[24] PBI-Ad-2 (13.7 wt % for CO_2 uptake, 1.3 wt % for H_2 uptake, 926 $m^2 g^{-1}$)[19] and CMP-1 (9.02 wt % for CO_2 uptake, 1.01 wt % for H_2 uptake, 837 $m^2 g^{-1}$).[25] Additionally, in our previous works, we reported two series of microporous organic polymers, MOP-Ads[15] and HBPBAs,[16] which exhibited similar BET surface areas but lower gas uptake capacity. This superior performance could be attributed to the narrower pore-size distribution of these **CMF-Ad** frameworks herein, as well as the π-conjugated skeleton.[7]

The single component adsorption isotherms of CO_2, N_2 and CH_4 were used to evaluate the selectivities of CO_2 over N_2 and CH_4, calculated from Henry's law at 273 K and low pressure (less than 0.15 bar) (ESI, Fig. S10).[1] As shown in the Table S3 (ESI), the three networks exhibited ultra-high CO_2 selectivity over N_2, which was up to 41.7, 33.3 and 33.1, respectively. These results may be attributed to the higher polarizability value (26.3×10^{-25} cm^3) and larger quadrupole moment (4.30×10^{-26} esu^{-1} cm^{-1}) of CO_2 than N_2 (polarizability value = 17.6×10^{-25} cm^3; quadrupole moment = 1.52×10^{-26} esu^{-1} cm^{-1}).[8, 26, 27] Additionally, the extended conjugated π-electron structure in polymers has been demonstrated to interact with the quadrupole moment of CO_2, which would also result in excellent CO_2 uptake capacities.[7, 28] It is interesting that these CO_2/N_2 selectivity values are comparable to conjugated microporous frameworks reported, such as CMP-SO-1B2 (19.2),[29] PHCTF-6 (22),[30] Ad-L CTFs (13-20),[31] InCz-HCPs (26.5-29.0)[32] and CB-PCP-1 (9.02).[33] This result can be ascribed to the smaller sized pores of the **CMF-Ad** herein, which could tend to be more effective for CO_2 (3.30 Å) capture over large gas molecules such as N_2 (3.64 Å) and CH_4 (3.82 Å) at low pressure due to the molecular seizing effect.[30, 34]

Additionally, the CO_2/CH_4 selectivities for the three **CMF-Ad** networks were 4.2, 3.6 and 5.4, respectively. Generally, gas capacities decrease as the BET surface area of the microporous framework decreases. Interestingly, **CMF-Ad-3** exhibited the lowest CO_2 and CH_4 uptake capacities, but highest CO_2/CH_4 selectivity compared with **CMF-Ad-1** and **CMF-Ad-2**. This could be attributed to the abundant π-conjugated skeleton of the **CMF-Ad-3** networks (enhanced by the presence of alkyne linkages), enabling a high CO_2 capacity, even with a low BET surface area. As a result, **CMF-Ad-1** obtained the highest gas uptake capacity but **CMF-Ad-3** exhibited the best CO_2/CH_4 selectivity.[35, 36] Crucially, these findings suggest that both porous properties and the π-conjugated skeleton play pivotal roles in gas uptake.

In order to investigate the π-π interactions between adsorbent and adsorbate, the adsorption behavior of organic vapors (benzene and hexane) were also performed. All three **CMF-Ad** networks exhibited excellent vapor

uptake (up to 646 mg g^{-1} for benzene and 586 mg g^{-1} for hexane) at 298 K and P/P_0 = 0.8, comparable with, or superior to, most microporous organic polymers (ESI, Fig. S11 and Table S4).[16, 37, 38] According to Table S4 and Fig. S11 (ESI), **CMF-Ad-2** exhibited the highest benzene vapor uptake (646 mg g^{-1}) among the three frameworks, which is attributed to the higher relative content of phenyl groups in **CMF-Ad-2** (87.3 %) than **CMF-Ad-1** (82.1 %) and **CMF-Ad-3** (79.9 %). However, compared with **CMF-Ad-1**, **CMF-Ad-3** possess higher benzene vapor uptake, which was up to 594 mg g^{-1}. This could be attributed to the presence of alkyne groups (8.5 %) in **CMF-Ad-3**, which provides additional affinity sites for aromatic (benzene) molecules through strong π-π interactions.[8] Similarly, benzene vapor uptake for these three frameworks were much lower than previously reported PAF-11 (874 mg g^{-1} for benzene, 704 m^2 g^{-1}),[17] which is in line with PAF-11 containing a higher content of phenyl groups (96.2 %). On the other hand, large microporous pore volume plays a significant role in the enhancement of organic vapor sorption capacity.[19] As summarized in Table S2 (ESI), **CMF-Ad-2** displayed higher microporous pore volume (0.32 cm^3 g^{-1}) than **CMF-Ad-1** (0.26 cm^3 g^{-1}) and **CMF-Ad-3** (0.15 cm^3 g^{-1}). Accordingly, **CMF-Ad-2** possess the highest hexane vapor adsorption capacity (586 mg g^{-1}) and following were **CMF-Ad-1** (336 mg g^{-1}) and **CMF-Ad-3** (222 mg g^{-1}). Besides, the **CMF-Ad** networks showed lower hexane vapor adsorption capacity than benzene due to the lack of π-π interactions between the framework skeleton and hexane vapor. The high vapor adsorption capacities of these **CMF-Ad** networks are of considerable importance in the recovery and selective removal of toxic organic vapors from polluted air.

Conclusions

In summary, we have used a novel TBBPA knot in the preparation of a series of porous and conjugated microporous frameworks based on adamantane (**CMF-Ad**) *via* Suzuki coupling. Noticeably, owing to the π-electron-rich building blocks, our three **CMF-Ad** networks manifested not only extremely high physicochemical stability, but also excellent gas and organic vapor uptake capacities. The combination of large π-electron-rich skeletons, high thermochemical stability, high gas and organic vapor adsorption capacities renders these CMFs as promising materials for application in carbon dioxide capture and sequestration (CCS) and removal of volatile organic compounds (VOCs) from polluted environments.

Acknowledgements

This work was supported by National Natural Science Foundation of China (No. 21476051), Science and Technology Program of Guangdong Province (No. 2016A050502057), Science and Technology Program of Guangzhou City (No. 201704030075 and No. 201604010015) and Natural Science Foundation of Guangdong Province (No. 2016A030310349). PDT thanks the State Administration for Foreign Experts Affairs and the Royal Society of Chemistry for a Visiting Researcher Programme grant to China.

Notes and refernences

1. Y. F. Zhao, X. Liu and Y. Han, *RSC Adv.*, 2015, **5**, 30310-30330.
2. G. Y. Li, B. Zhang, J. Yan and Z. G. Wang, *Macromolecules.*, 2014, **47**, 6664-6670.
3. N. Hedin, L. Andersson, L. Bergström and J. Y. Yan, *App. Energ.*, 2013, **104**, 418-433.
4. A. G. Slater and A. I. Cooper, *Science*, 2015, **348**, 8075.
5. Y. H. Xu, S. B. Jin, H. Xu, A. Nagai and D. L. Jiang, *Chem. Soc. Rev.*, 2013, **42**, 8012-8031.
6. A. Bhunia, D. Esquivel, S. Dey, R. Fernandez-Teran, S. Inagaki, P. V.D. Voort and C. Janiak, *J. Mater. Chem. A.*, 2016, **4**, 13450-13457.
7. V. M. Suresh, S. Bonakala, S. Roy, S. Balasubramanian and T. K. Maji, *J.Phys. Chem.*, 2014, **118**, 24369-24376.
8. J. Yan, B. Zhang and Z. G. Wang, *Polym. Chem.*, 2016, **7**, 7295-7303.
9. Q. Chen, M. Luo, T. Wang, J. X. Wang, D. Zhou, Y. Han, C. S. Zhang, C. G. Yan and B. H. Han, *Macromolecules*, 2011, **44**, 5573-5577.
10. K. Y. Yuan, C. Liu, J. H. Han, G. P. Yu, H. M. Duan, Z. G. Wang and X. G. Jian, *RSC Adv.*, 2016, **6**, 12009-12020.
11. L. Pan, M. Y. Xu, L. J. Feng, Q. Chen, Y. J. He and B. H. Han, *Polym. Chem.*, 2016, **7**, 2299-2307.
12. Q. Chen, D. P. Liu, J. H. Zhu and B. H. Han, *Macromolecules*., 2014, **47**, 5926-5931.
13. R. S. Sprick, B. Bonillo, M. Sachs, R. Clowes, J. R. Durrant, D. J. Adams and A. I. Cooper, *Chem. Commun.*, 2016, **52**, 10008-10011.
14. L. Qin, G. J. Xu, C. Yao and Y. H. Xu, *Polym. Chem.*, 2016, **7**, 4599-4602.
15. X. Li, J. W. Guo, H. B. Yue, J. W. Wang and P. D. Topham, *RSC Adv.*, 2017, **7**, 16174-16180.
16. J. W. Guo, X. F. Lai, S. Q. Fu, H. B. Yue, J. W. Wang and P. D. Topham, *Mater. Lett.*, 2017, **187**, 76-79.
17. L. Qin, G. J. Xu, C. Yao and Y. H. Xu, *Chem. Commun.*, 2016, **52**, 12602-12605.
18. Y. Yuan, F. Sun, H. Ren, X. Jing, W. Wang, H. Ma, H. Zhao and G. Zhu, *J. Mater. Chem.*, 2011, **21**, 13498-13502.
19. B. Zhang, G. Y. Li, J. Yan and Z. G. Wang,. *J. Phys. Chem. C.*, 2015, **119**, 13080-13087.

20. H. Furukawa and O. M. Yaghi, *J. Am. Chem. Soc.*, 2009, **131**, 8875-8883.
21. D. Z. Tan, W. N. Xiong, H. X. Sun, Z. Zhang, W. Ma, C. G. Meng, W. J. Fan and A. Li, *Micropor. Mesopor. Mat.*, 2013, **176**, 25-30.
22. X. W. Jiang, Y. F. Liu, J. Liu, X. H. Fu, Y. L. Luo and Y. N. Lyu, *New J. Chem.*, 2017, **41**, 3915-3919.
23. J. J. Chen, T. L. Zhai, Y. F. Chen, S. N. Geng, C. Yu, J. M. Liu, L. L. Wang, B. Tan and C. Zhang, *Polym. Chem.*, 2017, **8**, 5533-5538.
24. R. Dawson, E. Stöckel, J. R. Holst, D. J. Adams and A. I. Cooper, *Energy. Environ. Sci.*, 2011, **4**, 4239-4245.
25. J. X. Jiang, F. B. Su, A. Trewin, C. D. Wood, H. J. Niu, J. T. A. Jones, Y. Z. Khimyak and A. I. Cooper, *J. Am. Chem. Soc.*, 2008, **130**, 7710-7720.
26. J. Liu, Y. F. Liu, X. W. Jiang, Y. L. Luo and Y. N. Lyu, *Micropor. Mesopor. Mat.*, 2017, **250**, 203-209.
27. J. Li, G. P. Yang, L. Hou, L. Cui, Y. P. Li, Y. Y. Wang and Q. Z. Shi, *Dalton T.*, 2013, **42**, 13590-13598.
28. A. M. Plonka, D. Banerjee, W. R. Woerner, Z. J. Zhang, N. Nijem, Y. J. Chabal, J. Li and J. B. Parise, *Angew. Chem. Int. Ed.*, 2013, **52**, 1692-1695.
29. Y. Yuan, H. L. Huang, L. Chen and Y. L. Chen, *Macromolecules.*, 2017, **50**, 4993-5003.
30. K. Y. Yuan, C. Liu, L. H. Zong, G. P. Yu, S. L. Cheng, J. Y. Wang, Z. H. Weng and X. G. Jian, *ACS Appl. Mater. Inter.*, 2017, **9**, 13201-13212.
31. S. Dey, A. Bhunia, I. Boldog and C. Janiak, *Micropor. Mesopor. Mat.*, 2017, **241**, 303-315.
32. D. Chang, M. Yu, C. Zhang, Y. Zhao, R. Kong, F. Y. Xie and J. X. Jiang, *Micropor. Mesopor. Mat.*, 2016, **228**, 231-236.
33. A. Dani, V. Crocellà, C. Magistris, V. Santoro, J. Y. Yuan and S. Bordiga, *J. Mater. Chem. A.*, 2017, **5**, 372-383.
34. J. Germain, F. Svec and J. M. J. Fréchet, *Chem. Mater.*, 2008, **20**, 7069-7076.
35. Y. H. Xu and D. L. Jiang, Chem. Commun., 2014, 50, 2781-2783.
36. J. R. Li, R. J. Kuppler, H. C. Zhou. *Chem Soc Rev*, 2009, **38**, 1477-1504.
37. H. Ren, T. Ben, E. S. Wang, X. F. Jing, M. Xue, B. B. Liu, Y. Cui, S. L. Qiu and G. S. Zhu, *Chem. Commun.*, 2010, **46**, 291-293.
38. H. Yu, M. Z. Tian, C. J. Shen and Z. G. Wng, *Polym. Chem.*, 2013, **4**, 961-968.